International Journal of Pharmacognosy and Clinical Research

ISSN Print: 2664-763X
ISSN Online: 2664-7648
Impact Factor: RJIF 8.25.
IJPCR 2026; 8(1): 01-16
www.pharmacognosyjournal.in
Received: 02-11-2025
Accepted: 05-12-2025

Nisha Grewal
Faculty of Pharmaceutical Sciences, Baba Mastnath University, Rohtak, Haryana, India

Balvinder Singh
Faculty of Pharmaceutical Sciences, Baba Mastnath University, Rohtak, Haryana, India

Corresponding Author:
Balvinder Singh
Faculty of Pharmaceutical Sciences, Baba Mastnath University, Rohtak, Haryana, India

Advanced lipid-based nanocarriers for cutaneous fungal infections: A pharmaceutical design and *In vitro* evaluation of antifungal nanostructured lipid carriers

Nisha Grewal and Balvinder Singh

DOI: https://www.doi.org/10.33545/2664763X.2026.v8.i1a.82

Abstract
Introduction: Fungal infections represent a significant concern to worldwide public health, as the rise of antifungal resistance constrains current therapy choices. Sulconazole nitrate (SCZ), an antifungal drug, may be regarded as a viable candidate for effective transdermal delivery. This study aimed to design and assess SCZ nanostructured lipid carriers (NLCs) for enhanced skin penetration and therapeutic effectiveness.
Methods: The preformulation studies encompass drug identification, solubility assessment, UV and IR analysis, and partition coefficient determination. Lipids were evaluated for solubility in SCZ, leading to the selection of solid (stearic acid) and liquid (isopropyl myristate) lipids deemed most suitable. NLCs were synthesized using a modified microemulsion technique and statistically optimized by Central Composite Design. Essential factors, including particle size, zeta potential, and entrapment efficiency, were analyzed utilizing photon correlation spectroscopy (PCS) and scanning electron microscopy (SEM) methodologies. The optimized formulation was assessed for stability for a period of 180 days.
Results: Optimized formulation (NLC-SN10) showed mean particle size of 395.24 ± 2.46 nm, entrapment efficiency of 76.14 ± 1.35%, and zeta potential of −23.85 ± 0.25 mV. Spherical shape was confirmed by SEM. Stability studies showed minimal change in particle size, zeta potential, and drug entrapment, making the formulation stable for six months.
Conclusion: SCZ-loaded NLCs showed considerably higher drug entrapment and stability, which also signaled their potential in amplified topical antifungal therapy. The formulation had great physicochemical and biological attributes, which also signaled potential for extra clinical study.

Keywords: Sulconazole nitrate, Nanostructured lipid carriers, Antifungal therapy, Topical gel, Entrapment efficiency, Skin delivery

Introduction
Fungal infections continue to pose a significant threat to global health, with various forms - ranging from superficial to systemic impacting people worldwide. Deficiencies of existing antifungal drugs, however effective if we evaluate the benefits and dangers, are associated with undesirable effects such as hepatotoxicity and interference in estrogen metabolism that can be associated with allergic reactions and other toxicities [1]. SCZ is a medication having a wide range of action and antifungal, antiparasitic, antibacterial, and even anticancer properties. It inhibits the manufacture of ergosterol, an important portion of the fungal cell lipid layer, which is necessary for the preservation of the cell's membrane [2]. The anti-parasitic actions of SCZ are attributable to its powerful suppression of cytochrome P450 enzymes, which are important for the survival of protozoa and helminths [3]. Its antibacterial activity is likely related to suppression of flavoHb and enzyme disruption (e.g., DNA gyrase and topoisomerase IV) [4]. On a worldwide basis, invasive fungal infections continue to make a considerable contribution towards infectious illness-linked death, with Candida species, principally C. albicans, being the leading cause of invasive candidiasis. Since fungi have a plethora of biological features in common with human cells, possibilities for treatment are restricted. Currently, there are only three major classes of antifungal medications accessible, and the efficiency is challenged by the development of resistant strains [5].

To address these hurdles, a focus on improving the effectiveness of current antifungal medicines is necessary. Therefore, the originality of the present study lies in improving dermal delivery of SCZ by driving its entrapment into NLCs with a potentially improved therapeutic effect. The present inquiry is aiming to create and characterize a topical gel formulation loaded with SCZ-NLCs for both in vitro and in vivo experiments. NLCs, an advanced lipid carrier system, have been developed on solid-liquid combination lipids [6]. These lipidic formulations are biodegradable, and the composition is remarkably close to that of human stratum corneum as well as sebum, which decreases adverse effects risk [7]. NLCs have a lower melting point and solidify at room temperature due to the presence of liquid lipids [8]. Solid lipids (in NLCs) have delayed drug release, and lowering systemic drug exposure by the usage on the skin evokes an occlusive action [9, 10]. Due to increased solubility of the drug in mixed lipids, the drug entrapment within NLCs is higher than that in solid lipid nanoparticles [11]. Furthermore, such nano-sized particles promote adhesion to the stratum corneum that allows for deeper percutaneous drug absorption into the skin. In recent years, NLCs have drawn great attention in cosmetics, medicines, and functional foods; much promise for future commercial application has been revealed [12]. The three-dimensional framework is obtained from the inorganic phase, and gel formulations, which are well-known in the field, preserve a semisolid composition with both organics and inorganics suspended within a liquid matrix for topical application [3]. Such gels are envisaged to be non-greasy in nature, washable, stable at room temperature, and inert with respect to the biological activity of the medication [14].

2. Materials and Methods

Sulconazole nitrate (SCZ) was procured as a complimentary sample from Elegant Pharma Pvt. Ltd. (Karnataka, India). Chemicals such as cetyl palmitate, acetonitrile, caprylic acid, acetic acid isopropyl myristate, propylene glycol (PG), oleic acid, polyethylene glycol 400 (PEG 400), Tween 80, triethanolamine, potassium dihydrogen phosphate, disodium hydrogen phosphate, methanol and chloroform were sourced from S. D. Fine Chemicals Ltd., Mumbai, India. HPLC-grade methanol and phosphoric acid were sourced from Sigma Aldrich Co. Ltd., USA. Sodium chloride was supplied by E. Merck India Ltd.

2.1 Pre-formulation Research

Initial studies were undertaken to evaluate SCZ through identification and partition coefficient analyses. The findings were assessed in accordance with established pharmacopeial references and documented literature.

2.1.1 Drug Identification

The identification of SCZ involved an assessment of its physicochemical parameters, including solubility profile, melting point, ultraviolet (UV) spectral analysis as well as infrared (IR) spectroscopy [15].

2.1.1.1 Physical Characteristics

The appearance of SCZ were observed visually for consistency and conformity with reference standards.

2.1.1.2 Melting Point

A capillary tube sealed at one end was filled with a minute amount of SCZ. The temperature when the drug started to melt was noted when this tube was put in a melting point apparatus [16].

2.1.1.3 Solubility

The solubility of SCZ was determined in different solvents, including water, methanol, acidic medium, and basic medium. A 0.0015% w/v methanolic solution of SCZ was prepared and analyzed using a UV spectrophotometer (Hitachi U-2800, Tokyo, Japan) within the wavelength range of 230-380 nm, and the wavelength corresponding to maximum absorption (λmax) was identified.

2.1.2 Estimation of SCZ by UV Spectrophotometry

A calibration curve for SCZ was constructed in methanol by analyzing standard solutions at the identified λmax using a UV spectrophotometer. Ten milligrams of SCZ were dissolved in a small quantity of methanol in a 100ml volumetric flask, then diluted to volume to get a stock solution of 100 µg/ml. Dilutions in series of 2 to 20 µg/ml were prepared by transferring specific volumes (0.2 to 2.0 ml) into different 10 ml volumetric flasks and diluting with methanol. The absorbance for each solution was record at 450 nm by using a Hitachi U-2800 UV spectrophotometer. The resulting data were analyzed statistically using Microsoft Excel [17].

2.1.3 Infrared (IR) Spectroscopy

For IR analysis, SCZ was blended with IR-grade KBr in a 1:10 ratio, and pellets were formed using a KBr press (Spectra Labs, Mumbai, India). The IR spectra were record using a Perkin Elmer FTIR spectrophotometer (Germany) and compared against the British Pharmacopoeia 2023 reference spectra [18].

2.1.4 Calibration Curve via HPLC

Two milligrams of SCZ were accurately weighed and dissolved in a mixture of methanol, water, and phosphoric acid in the ratio of 69.9:30:0.1, forming a 100 ml stock solution at 20 µg/ml concentration. Dilutions ranging from 0.2 to 2.0 µg/ml were prepared from the stock by drawing 0.2 to 2.0 ml aliquots and dilute to 10 ml of mobile phase. These were analyzed using HPLC, with 20 µl sample injections and flow rate of a mobile phase is 1 ml/min. At 450 nm UV detection was set and performed at room temperature. Areas of peak were plot against concentrations to generate calibration curve. Each trial was conducted thrice to ensure reliability [19].

2.1.5 Partition Coefficient Determination

SCZ's partition coefficient was evaluated in phosphate buffer saline (PBS, pH 7.4) which was saturated with n-octanol. To equilibrate, PBS and n-octanol were stirred for 24 hours. Each vial contained 10 ml each of PBS and n-octanol along with 10 mg of SCZ. For 72 hours, the vials were incubated in a shaker (Remi Equipments, Mumbai, India). After equilibrium was attained, phases get separated with the help of a separating funnel. The concentration of SCZ in each layer was examined by using a Hitachi U-2800 UV spectrophotometer at 450 nm [20].

$$\text{Partition coefficient} = \frac{cancentration\ of\ drug\ in\ n-octanol\ layer}{concentration\ of\ drug\ in\ phosphate\ buffer\ layer}$$

2.2. Screening of Lipids and Surfactant

2.2.1 Lipid Screening

To determine the most suitable solid and liquid lipids for formulating nanostructured lipid carriers (NLCs), screening was conducted based on the drug's solubility in various lipids. For solid lipids with melting points above room temperature, solubility assessments were conducted in the molten state. Precisely 2 mg of each solid lipid was melted in glass vials by heating them 50°C above their melting point. SCZ nitrate was added in extra amount to each melted lipid to evaluate solubility. For liquid lipids, solubility studies were carried out by mixing an excess amount of SCZ nitrate with 5 ml of different lipids (caprylic acid, oleic acid and isopropyl myristate) in the screw-capped containers. These were kept at room temperature to equilibrate for 72 hours. Then the samples were centrifuged for 10 minutes at 3000 rpm. The resulting supernatants liquids were diluted appropriately with methanol. The concentration of SCZ nitrate was determined at 450 nm by using a UV spectrophotometer [21].

2.2.2 Miscibility of Solid and Liquid Lipids (Improving Internal Lipid Structure)

To establish an efficient lipid matrix for the NLC system, physical blends of solid and liquid lipids were prepared in the different ratios: 90:10, 85:15, 80:20, 75:25, 70:30, 65:35, and 60:40. Each mixture was tested with SCZ at three concentrations: 1%, 5%, and 10%. The drug SCZ nitrate and lipid amounts were weighed using an electronic weighing balance (Sartorious AG, Type L 2200P-xD2, Gottingen, Germany), then heated on a magnetic stirrer at 65°C for 1 hour. The solubility observations of SCZ were done visually using a binocular microscope at intervals of 20, 40, and 60 minutes while maintaining the samples at 65 °C. These samples were then cooled and examined again after 24 hours at room temperature [22].

2.2.3 Optimization

2.2.3.1 Optimization and Formulation of Sulconazole Nitrate NLCs

The optimization of the NLC formulation was carried out using Design Expert® software (trial version 11, USA), applying a Central Composite Design. The study focused on three key formulation parameters: Stearic acid amount (A), Isopropyl myristate amount (B), and Lecithin content (C). The selected ranges for optimization were: Stearic acid (700-850 mg), Isopropyl myristate (150-300 mg), and Lecithin (100-200 mg). The two major response variables considered were the mean particle diameter (d90%, R1) and encapsulation efficiency (R2). The objective was to determine optimal values for these parameters to enhance formulation performance. Table 1 includes a comprehensive summary of all combinations of independent and response variables in both coded and actual forms. The generated mathematical equations were used within the software to model and predict outcomes such as nanoparticle size and drug loading efficiency [23].

The NLC preparation involved heating Stearic acid and Isopropyl myristate above the melting point of Stearic acid that is 50°C. In a separate beaker, SCZ and Lecithin were dissolved and subsequently blended into the melted lipid mix. This drug-lipid blend was added to the aqueous phase dropwise that was contained Tween 80 (2% w/v), by continuous mechanical stirring, it forms a transparent and uniform emulsion.

The emulsion was then transferred to a chilled water bath at around 10°C and stirred at 5000 rpm for 2 hours. The cooling process caused the lipid droplets to solidify within the surfactant medium, effectively forming the NLCs. NLCs were stored at low temperatures for subsequent analysis. For the design, Stearic acid (A), Isopropyl myristate (B), and Lecithin (C) were studied at three levels: low (-1), medium (0), and high (+1), as detailed in Table 1. The influence of the above factors was evaluated on mean particle size in nm (R1) and drug entrapment efficiency in % (R2) [24, 25]. A total of 15 experimental runs were generated by the software, showing a combination of input values and responses as presented in Table 2.

Table 1: Independent Variables with level and response in central composite design of Sulconazole nitrate based NLC's

Variables (factors)	Level used		
Independent variables (factors)	**Low (-1)**	**Medium (0)**	**High (+1)**
A= Steric acid (mg)	700	800	900
B= Isopropyl myristate(mg)	150	200	250
C= Lecithin (mg)	100	150	200
Dependent variables (Response)	Minimize		
R_1 = Mean particle size (nm)			
R2=Drug Entrapment Efficacy (%)			

Table 2: Experimental Design Generated by Design Expert (Central Composite Design) of Sulconazole Nitrate Based NLC's

Formulation Code	Drug Content (mg)	Amount of Lipid (steric acid in mg)	Amount of Lipid Isopropyl myristate (mg)	Amount of Co-surfactant Lecithin (mg)	Tween 80 Surfactant %
NLC-SN1	100	780	150	180	2
NLC-SN2	100	850	180	180	2
NLC-SN3	100	900	200	200	2
NLC-SN4	100	950	180	180	2
NLC-SN5	100	980	180	180	2
NLC-SN6	100	1000	200	150	2
NLC-SN7	100	800	220	200	2
NLC-SN8	100	920	200	100	2
NLC-SN9	100	850	150	100	2
NLC-SN10	100	900	200	180	2
NLC-SN11	100	775	225	150	2
NLC-SN12	100	775	225	150	2
NLC-SN13	100	775	225	150	2
NLC-SN14	100	775	225	150	2
NLC-SN15	100	775	225	150	2

2.3. Formulation of SCZ-NLC

SCZ-NLCs were prepared by the reported method of Muller *et al*., 2000 with little modification [17]. The NLC dispersion with lipid phase (10%) was made using the micro emulsion template method with minimal adjustments. A known-composition lipid mixture (100 mg) was weighed accurately in a glass vial before being heated on a magnetic hot plate at temperature 65 °C. A preset quantity of filtered (0.22 m) water also added at 65°C to the melted material while being magnetically agitated to create homogenous, milky slurry. After adding a calculated volume of PG and Tween 80 to the homogenate, it was combined (total volume = 1 ml). The quick formation of the micro emulsion made the liquid transparent in a few seconds. The warm micro emulsion precursor was cooled in the same container at room temperature to harden the lipid matrix and subsequently produced NLC dispersion. The lipid phase was replaced with a precise amount of SCZ to produce the drug-loaded NLC [26].

2.4 SCZ-NLCs Characterization

2.4.1 Scanning Electron Microscopy

Additional information was gathered through SEM analysis to study the particle size and shape, particularly focusing on spherical and disc-like particles falling within the nanometer range. The size measurement being conducted using Malvern mastersizer. The SEM images revealed clusters of particles, attributable to the carrier's polymorphic nature and the specific sample preparation method used for microscopic assessment [27].

2.4.2 Analysis of Zeta Potential and Particle Size

Photon correlation spectroscopy (PCS) was employed to determine the particle size distribution and polydispersity index (PDI) of the formulations. Prior to measurement, the samples were diluted ten-fold with double-distilled water to achieve an appropriate scattering intensity. Zeta potential (ZP) measurements were performed at 25 °C under an applied electric field of approximately 24.60 V/cm. Before analysis, the conductivity of the samples was adjusted to 50 mS/cm using a 0.1 mM NaCl solution [28].

2.4.3 Drug entrapment efficiency

After extracting the free drug using ultra-dialysis against an acetate buffer (pH 6.0) having 30% PEG 400 (v/v) for 4 hours at 4°C in a dialysis bag, the amount of drug trapped in the formulation was calculated. The dialyzed formulation was lysed with Triton-X 100 (0.1% v/v) before being examined by UV spectro-photometry at 430 nm for the presence of the drug (A2). Equation used to calculate the drug entrapment efficiency percentage (% E.E) [27].

$$EE(\%) = \frac{A2}{A1} \times 100$$

Where, A1 is the total amount of drug added in the formulation.

3. Results and Discussion

3.1 Pre-formulation studies

3.1.1 Drug characterization

The gifted sample of Sulconazole from Elegant Pharma Pvt Ltd Bangalore was characterized by Aspects to consider include appearance, melting point, solubility, and capturing UV and IR absorption spectra. Table 3 shows the results of pre formulation study.

Table 3: Results of Pre Formulation Study

Sr. No	Test	Observation	Inferences
1	Appearance	It is white to off white crystalline powder	White crystalline powder
2	Melting Point	130-132 ℃	131.5℃ ±1.09℃
3	Solubility	Partially soluble in water and completely soluble in Alcohol, Acetone and chloroform	Soluble in organic solvent
4	Absorption maxima	450 nm	449.86 nm

3.1.2 Ultraviolet spectroscopy: The 0.002% w/v solution in methanol displayed absorption maxima at 449.86 nm when evaluated in between the range of 200 nm to 550 nm. Figure 1 shows the UV-Visible spectrum of Sulconazole nitrate.

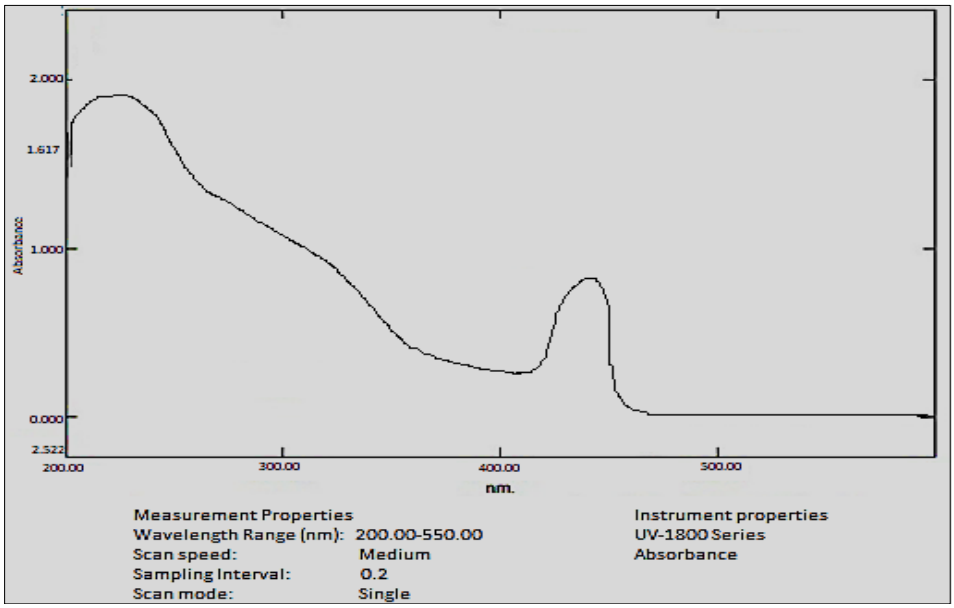

Fig 1: UV-Visible Spectrum of Sulconazole Nitrate

3.1.3 FT-IR Spectroscopy: FT-IRspectrum of pure sulconazole nitrate sample shows a N-H stretch at 3503.03 cm^{-1}, aromatic stretching at 3337.18cm^{-1}, aliphatic stetching 3012.28cm^{-1}, -S- thionyl stretching 2642.28cm^{-1} alkane CH_2 stretching 958.75cm^{-1} and -Cl stretching 745.09cm^{-1}. The absorption peaks were identical to the reported (I.P.2023), confirming the identity of Sulconazole nitrate. Figure 2 shows the FT-IR Spectrum of SCZ.

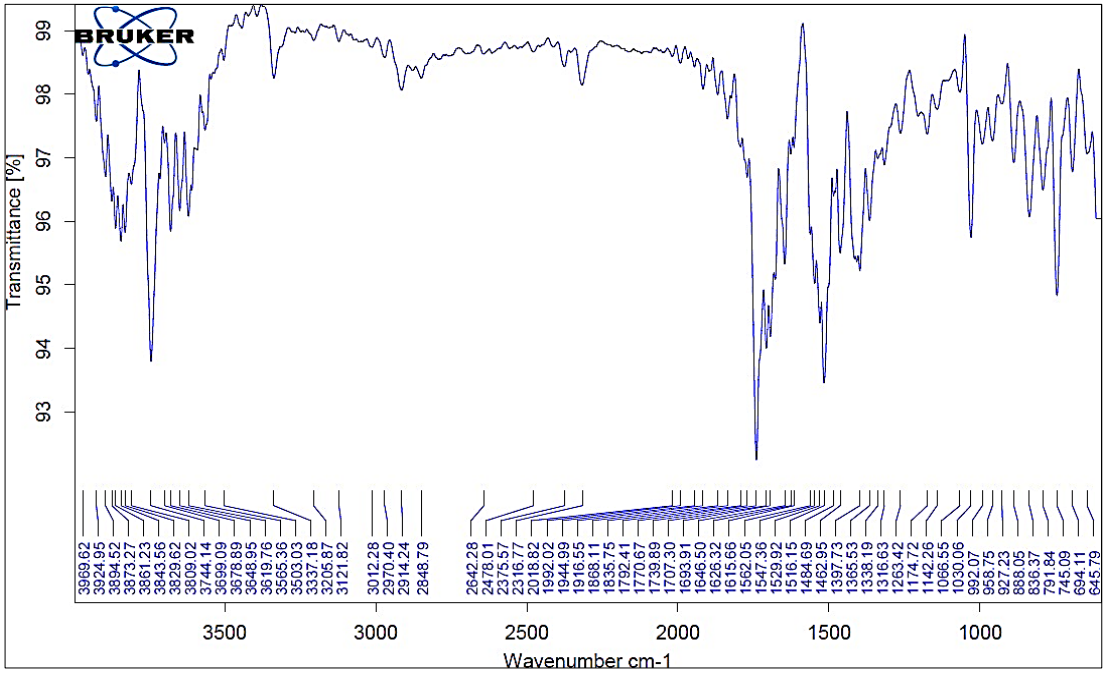

Fig 2: FT-IR Spectrum of Sulconazole Nitrate

The sample approximately 1-2 mg was thoroughly blended with potassium bromide (anhydrous) in preparation for the infra-red spectroscopy study, a crucial step in analyzing the chemical composition of lipids. The examination of FTIR spectra focused on various lipid combinations such as steric acid (SA), SA+ Isopropyl myristate (IM), SA+SCZ, SA+SCZ+IM, and SCZ+NLC presenting a comprehensive overview of their molecular structures. Upon comparing the spectra from figures 3 to 7, it was evident that there were no substantial deviations in the key peaks observed between the SCZ spectrum and the diverse spectrums of physical mixtures. This noteworthy observation provided strong evidence supporting the notion that there exists a high level of physical compatibility between the active pharmaceutical ingredient SCZ and the excipients utilized in the formulation. Furthermore, the consistent absence of significant disparities in the SCZ peaks when juxtaposed with the various physical mixtures served to reinforce the conclusion regarding the seamless integration of the drug with the accompanying formulation components. These compelling results not only validate the successful amalgamation of the drug with its surrounding excipients but also highlight the promising synergy achieved within the formulation, signifying a harmonious and effective blend of all constituents involved in the pharmaceutical product development process.

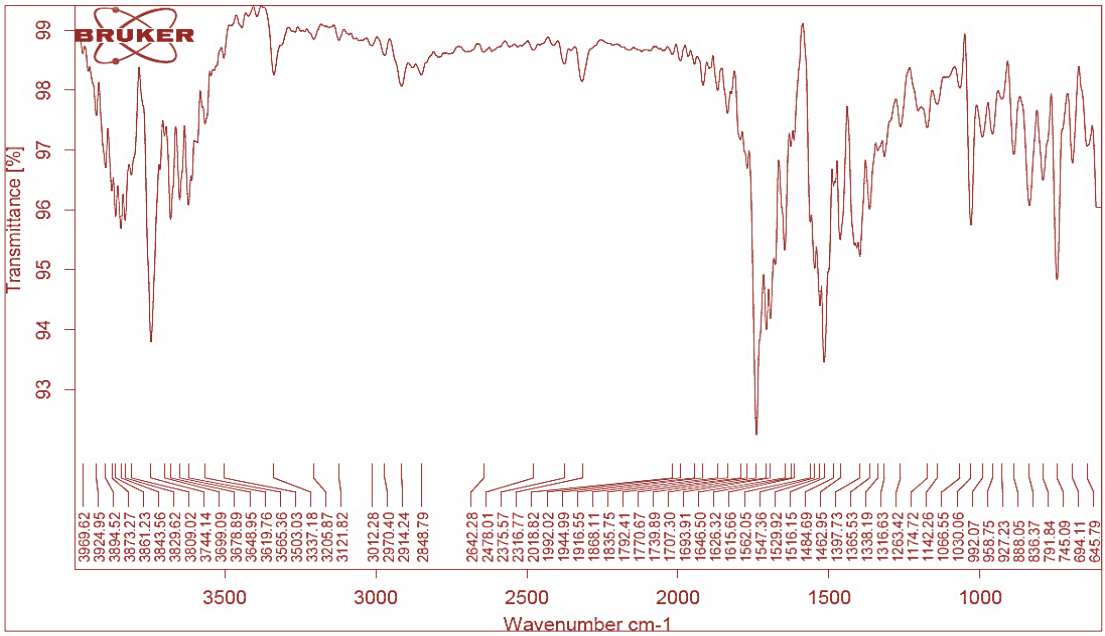

Fig 3: FT-IR Spectrum of Steric Acid (SA)

Fig 4: FT-IR Spectrum of Steric Acid (SA) + Isopropyl Myristate (IM)

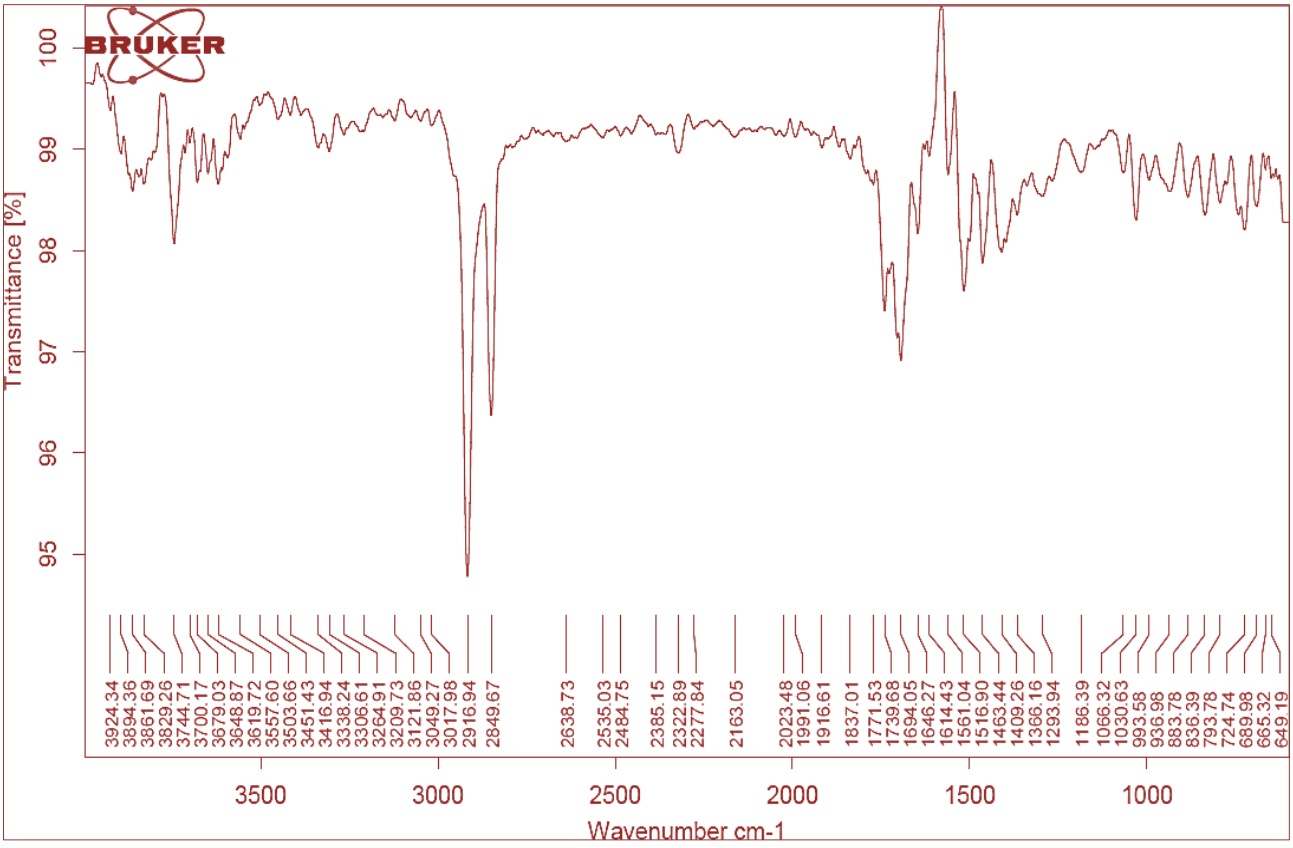

Fig 5: FT-IR Spectrum of Steric Acid (SA) + SCZ

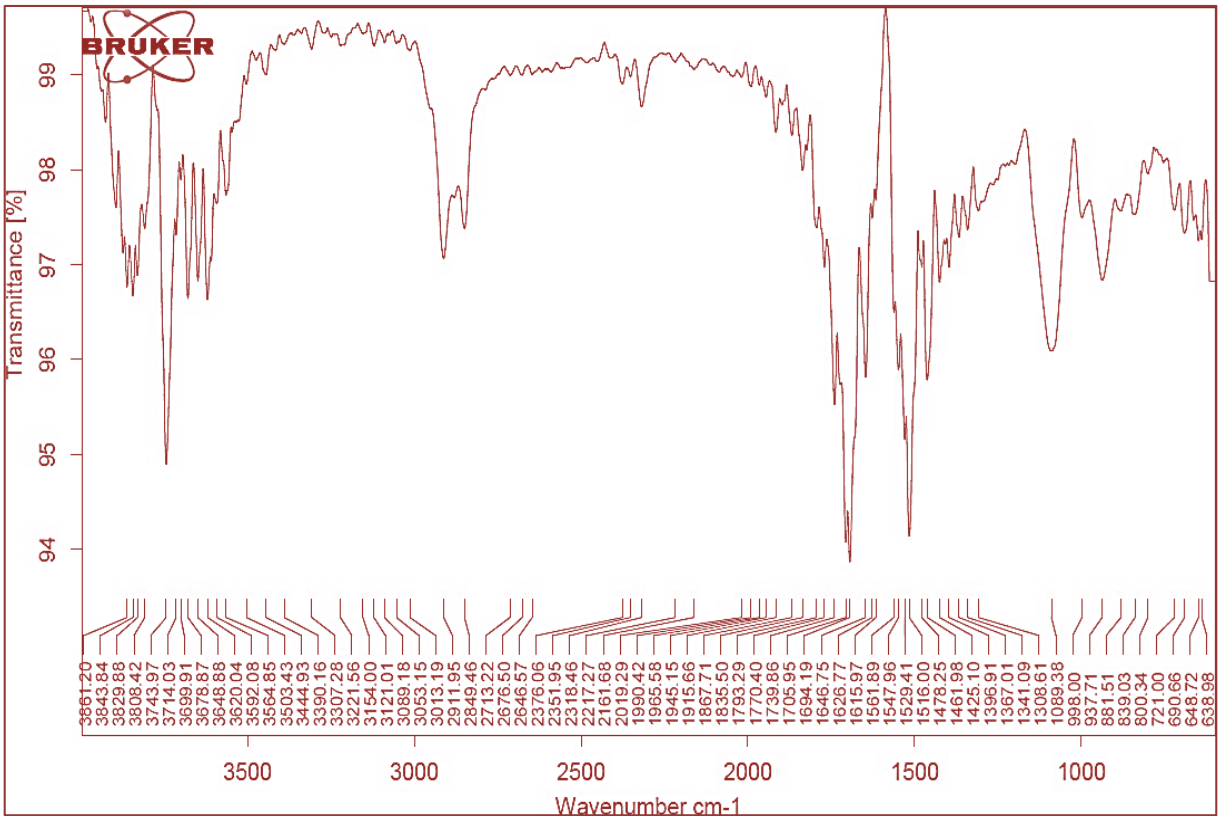

Fig 6: FT-IR Spectrum of Steric Acid (SA) + Isopropyl Myristate (IM) + SCZ

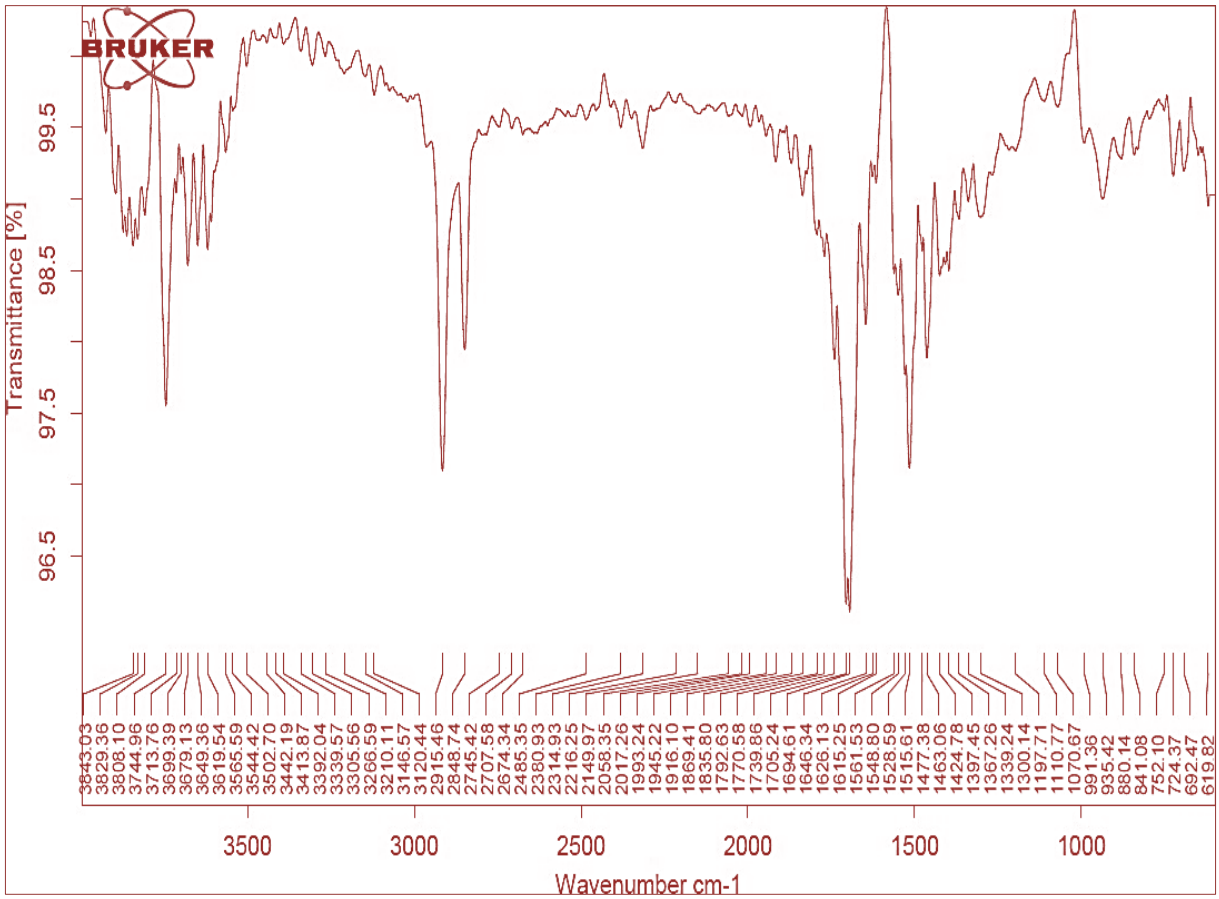

Fig 7: FT-IR Spectrum of SCZ + NLC

3.1.4 Calibration Curve Preparation

3.1.4.1 *In-vitro* Drug Release and Standard Calibration Curve: Calibration curves of sulconazole were prepared in different phosphate buffer solutions using a predetermined method to obtain varying concentrations. The regression equation was derived considering solubility, partition coefficient, and in-vitro drug release studies. The correlation coefficients (R^2 values) are presented in Tables 4-7, and the

corresponding calibration curves are illustrated in Figures 8- 11.

Table 4: Data for Calibration Curve of Sulconazole at 450nm in PBS pH 4.0 For Solubility Study

Sr. No.	Concentration (µg/ml)	Absorbance at 450nm
1	2	0.223
2	4	0.364
3	6	0.572
4	8	0.790
5	10	0.956

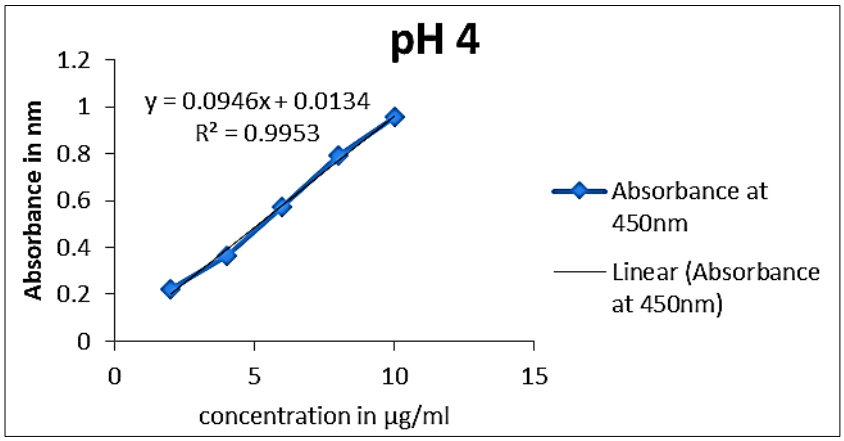

Fig 8: calibration curve of Sulconazole at 450nm in PBS pH 4.0 for Solubility study

Table 5: Data for Calibration Curve of Sulconazole at 450nm in PBS pH 5.0f or Solubility Study

Sr. No.	Concentration (µg/ml)	Absorbance at 450nm
1	2	0.210
2	4	0.420
3	6	0.635
4	8	0.845
5	10	0.959

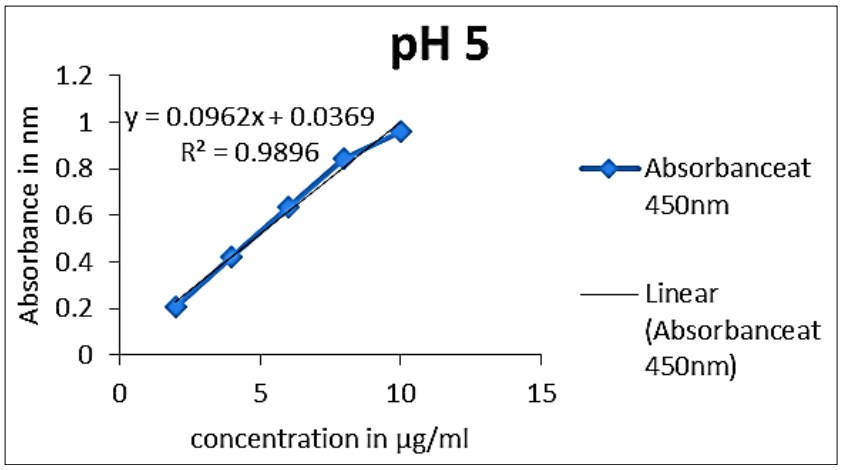

Fig 9: Calibration Curve of Sulconazole at 450nm in PBS pH 5.0 for Solubility Study

Table 6: Data for Calibration curve of Sulconazole at 450nm in PBS pH 6.0 for Solubility Study

Sr. No.	Concentration (µg/ml)	Absorbance at 450nm
1	2	0.196
2	4	0.445
3	6	0.620
4	8	0.834
5	10	0.985

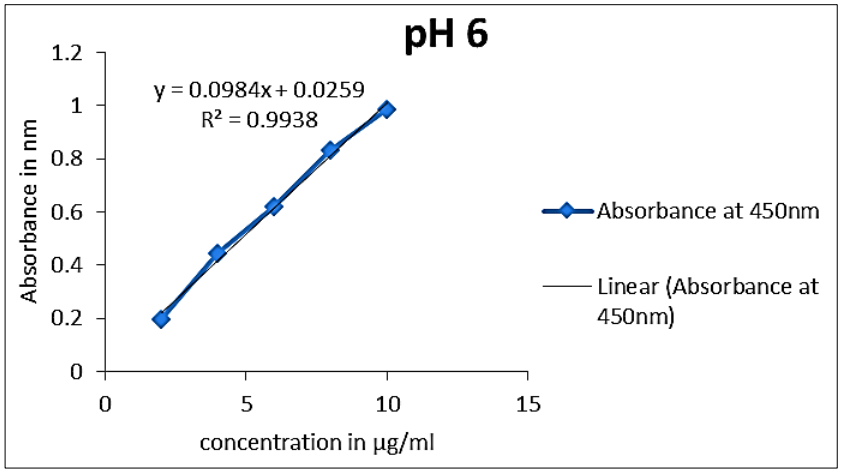

Fig 10: calibration curve of Sulconazole at 450nm in PBS pH 6.0 for Solubility study

Table 7: Data for Calibration Curve of Sulconazole at 450nm in PBS pH 7.0 for Solubility Study

Sr. No.	Concentration (µg/ml)	Absorbance at 450nm
1	2	0.194
2	4	0.482
3	6	0.568
4	8	0.828
5	10	0.967

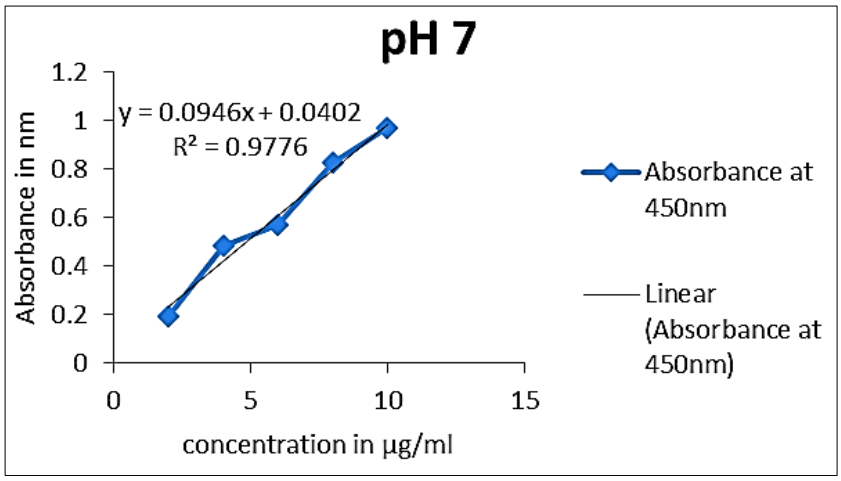

Fig 11: calibration curve of Sulconazole at 450nm in PBS pH 7.0 for Solubility study

3.1.5 Apparent Partition Coefficient of SCZ

Isopropyl myristate (IPM), which may replicate skin lipids by lowering the pH value, was selected to determine partitioning the lipophilic phase. The results of the apparent partition coefficient indicate an expected rise in the lipophilic characteristic of acidic medications like sulconazole. Despite the fact that the medication was completely ionized at pH 6.9, the partition coefficient is declining. This analysis demonstrated that the medication has managed lipoid and aqueous solubilities. As a result, the drug possibly will be considered a viable candidate for transdermal distribution because it is effectively solubilized in skin sebum and quickly permeates into the deeper skin layers to dissolve in the tissue fluids. **Table 8** shows the summarize results of partition coefficients.

Table 8: Apparent Partition coefficient of SCZ in Phosphate Buffer Solution

Sr. No.	System	Apparent Partition coefficient
1	IPM/ pH 4 Buffer	13.46±1.061
2	IPM/ pH 5 Buffer	10.13±0.56
3	IPM/ pH 6 Buffer	5.76±0.70
4	IPM/pH 7 Buffer	3.72±.46

*Mean ± S.D.(n=3)

3.2 Screening of Lipids and Surfactant

3.2.1 Selection of Solid Lipid

The drug's solubility in the lipid determines the lipid nanoparticle's encapsulation effectiveness in a nano formulation. It is anticipated that a high lipid solubility would lead to a high final formulation encapsulation efficiency. A variety of lipids were used in order to investigate the sulconazole's lipid solubility. Lipids having

melting points higher than room temperature require solubility analysis in the lipid melt. When compared to other lipids, stearic acid has the greatest capacity to solubilize sulconazole. The below graphic indicates the amount of solid lipid (measured in milligrams) needed to dissolve 10 milligrams of sulconazole in ascending order. Figure 12 shows the solubility results in different solid lipids.

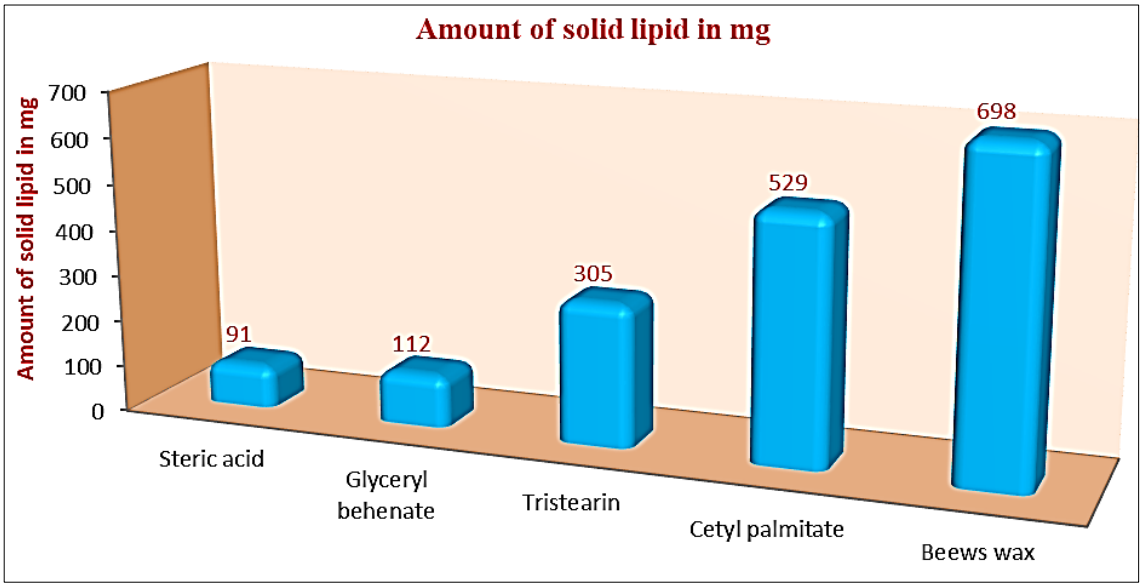

Fig 12: Solubility of Sulconazole in Different Solid Lipids

3.2.2 Selection of liquid lipid

The oils that were screened revealed that Isopropyl myristate had the highest solubility of Sulconazole, with Eucalyptus oil coming in second. Eucalyptus oil as a liquid lipid selected for the NLC formulation because it is one of the commonly used penetration enhancers in the semisolid vehicle applied to the skin, which may further enhance drug uptake. Figure 13 which shows the solubility of sulconazole nitrate in the different liquid lipids and surfactant.

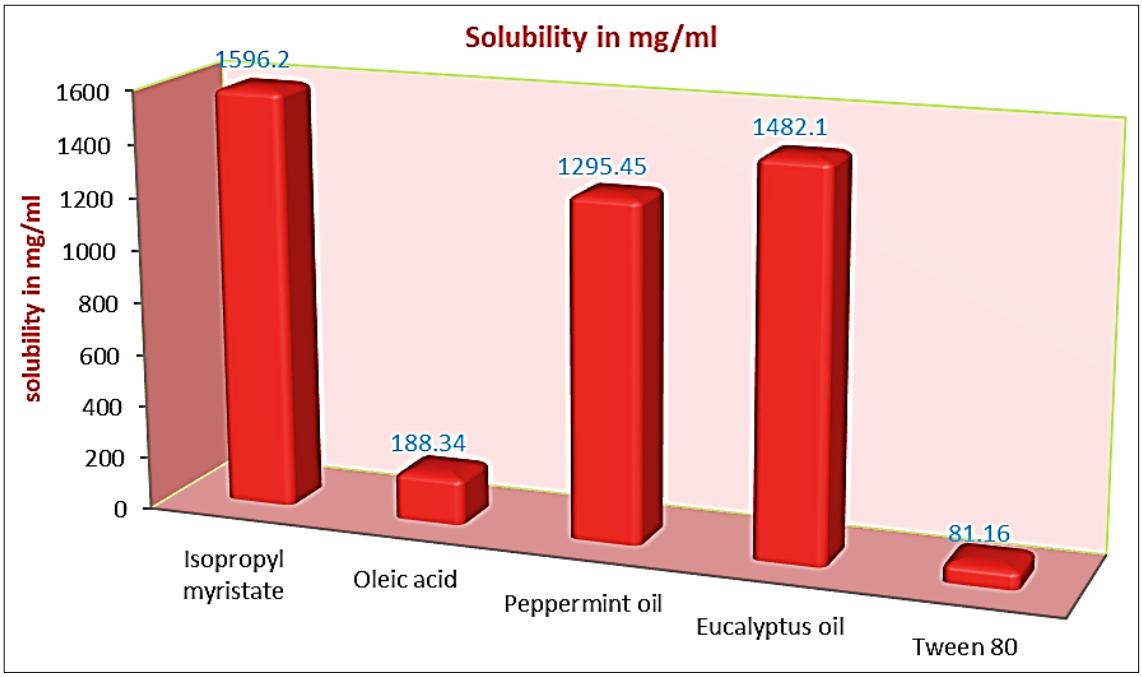

Fig 13: Solubility of SCZ in Different Liquid Lipids and Surfactant

3.2.3 Solid lipid and liquid lipid compatibility

After carefully selecting the solid lipid and liquid lipid components, a compatibility study was conducted to ascertain the interaction between the two lipids. Stearic acid and Isopropyl myristate were combined in a ratio of 9:1 and placed in glass vials, followed by heating at a temperature of 100 degrees Celsius. The mixture was assessed both promptly after solidification, as well as after a 24-hour period. Subsequent analysis revealed that the lipid combination exhibited a homogeneous single-phase behavior, confirming the successful compatibility between the solid and liquid lipids. This harmonious interaction serves as a critical foundation for the lipid selection process, highlighting the importance of achieving a unified lipid system for optimal product development.

3.3 Preparation of SCZ Loaded NLCS: The NLCs were successfully prepared using the modified microemulsion technique. Figure 14 show the formulation batches of SCZ laoded NLCs.

Fig 14: Formulation Batches of SCZ Laoded NLCs

3.4. Particle Size Distribution & Zeta Potential (ζ) of NLC Dispersion

The distribution of particle size values of nano-dispersion is detailed in the Table 9. Interestingly, it was observed that increasing the lecithin content resulted in a notable reduction in the particle size of the formulations. This decrease in size can be attributed to the particles separating without aggregating. Specifically, the particle size distribution d90% of the NLCs ranged from 400 to 700 nm. This distribution suggests that the majority, around 90%, of nanoparticles in the NLC-SN10 formulation are below the 400 nm threshold. This finding underscores the significant impact of lecithin on particle size in the nano dispersion, highlighting the importance of understanding and controlling formulation parameters for desired outcomes.

Table 9: Particle Size, Entrapment efficacy & Zetapotential of NLC Formulation

Formulation code	d90% Particle size	% EE	Zeta potential (mV)
NLC-SN1	542.21±3.40	68.34±1.05	-18.34±0.05
NLC-SN2	486.34±2.66	70.12±0.85	-20.36±0.56
NLC-SN3	520.40±1.75	66.45±1.74	-17.45±0.09
NLC-SN4	436.84±2.45	74.66±2.01	-22.78±0.01
NLC-SN5	425.94±1.25	75.44±0.08	-22.90±0.28
NLC-SN6	641.25±2.72	62.34±2.80	-16.45±0.34
NLC-SN7	574.34±1.37	69.34±2.16	-18.94±1.22
NLC-SN8	497.20±1.26	70.46±1.22	-21.05±0.54
NLC-SN9	445.31±1.70	71.42±1.05	-22.46±1.09
NLC-SN10	395.24±2.46	76.14±1.35	-23.85±0.25
NLC-SN11	441.21±2.40	66.24±1.35	-22.54±0.05
NLC-SN12	483.34±1.64	65.42±0.25	-22.56±0.96
NLC-SN13	425.40±2.75	64.33±1.04	-21.35±1.09
NLC-SN14	431.84±1.45	62.25±2.01	-21.78±1.01
NLC-SN15	428.94±1.25	65.74±0.18	-22.80±1.28

The evaluation of zeta potential was crucial for assessing the colloidal dispersion's long-term physical stability. In particular, the nano dispersion's higher zeta potential value was indicative of enhanced stability, with values above -30 mV demonstrating good stability levels. To ensure an extended shelf life, it was recommended that the optimized zeta potential of the formulation approach -60 mV. In our comprehensive study, the zeta potential of the various formulations, ranging from NLC-SN-1 to NLC-SN-15, was observed to fall within the range of -16.45 mV to -23.85 mV. Notably, further enhancements in formulation stability were achieved through the strategic coating of particles with a hydrophilic surfactant, forming an additional protective surface layer conducive to increased physical stability over time.

3.5 Optimization

The development of lipid nanoparticles can be described as a complex and intricate process, characterized by the interplay of various processing factors. These factors exhibit crucial interactions with each other, ultimately influencing the unique properties of the formulated products. In order to determine the influence of each factor on parameters such as mean size (Y1) and entrapment efficiency (Y2), ANOVA analysis was conducted. To identify the most appropriate model that elucidates the relationship in between the key components and outcomes, the collected data was fitted into

different models. After thorough evaluation, the 2FI model was selected based on its significant p-value from the analysis of the sum of squares and a non-significant lack of fit p-value for entrapment response when compared to the cubic, quadratic, and linear models. Thus, the 2FI model emerged as the most significant model to elucidate the effects of the factors on entrapment, providing valuable insights into the formulation process.

The model summary statistics for the response entrapment efficiency obtained through CCD of NLC. The linear model showed a standard deviation of 1.39 with an R^2 value of 0.3972, an adjusted R^2 of 0.3462, and a predicted R^2 of -0.1452. The 2FI model, which was suggested, demonstrated improved performance with a standard deviation of 1.18, an R^2 of 0.5961, an adjusted R^2 of 0.5735, and a predicted R^2 of -0.1942. The quadratic model showed a standard deviation of 1.17, with a higher R^2 value of 0.8421; however, the adjusted R^2 (0.6823) and predicted R^2 (-0.7234) indicated poorer predictive capability. The cubic model, which was aliased, exhibited the lowest standard deviation (0.0881) and the highest R^2 (0.9899), adjusted R^2 (0.9876), and predicted R^2 (0.9410), though its aliased nature limits interpretability.

Similarly, the model statistics for the response particle size via CCD of NLC. The linear model, suggested as the best fit, showed a standard deviation of 34.25, with R^2, adjusted R^2, and predicted R^2 values of 0.8740, 0.8164, and 0.7842, respectively. The 2FI model had a higher standard deviation of 37.64 and slightly increased R^2 (0.8764), but lower adjusted R^2 (0.8071) and predicted R^2 (0.6945). The quadratic model demonstrated improved precision with a standard deviation of 29.25 and higher R^2 (0.9423), although the adjusted R^2 (0.8545) and predicted R^2 (0.5671) indicated moderate predictive performance. The cubic model, which was aliased, showed the lowest standard deviation (17.80) and high R^2 (0.9891) and adjusted R^2 (0.9457); however, the predicted R^2 was negative (-0.1634), limiting its suitability for reliable prediction.

3.5.1 Effect on CCD on particle size (NLC Dispersion)

The particle size (average) of the NLC dispersion ranged from 400 nm to 700 nanometers, reflecting the varied values of independent variables. Notably, in the range of formulations, NLC-SN-10 exhibited the smallest particle size at 395nm, while NLC-SN-6 presented the largest at 641 nm. The impact of lipids and lecithin on nanoparticle size can be observed in the accompanying. When lipid and lecithin concentrations are low, the particle size tends to increase. In contrast, increasing lipid levels while decreasing lecithin levels led to the highest particle size of 641 nm. The inverse relationship between lecithin and lipid amounts was evident, as an increase in lecithin saw a reduction in particle size, coupled with a decrease in lipid content.

3.5.2 Effect of CCD on Entrapment Efficacy (NLC Dispersion): When examining the efficiency of Sulconazole entrapment in lipid-based nano formulations, it is essential to note that the entrapment efficacy values for each prepared nano dispersion ranged from 62.34% to 76.14%. The calculated R2 value of 0.6945 indicates that the model adheres to 2FI principles. Specifically, Formulation NLC-SN1, which contains 780 mg of lipid, was able to successfully entrap 68.34% of the drug, while Formulation NLC-SN10, with a higher lipid concentration of 900 mg, achieved an impressive 76.14% drug entrapment rate. These results signify the promising potential of Sulconazole entrapment within lipid-based nano formulations and highlight the importance of precise formulation techniques for optimizing drug entrapment efficiency.

3.5.3 Point Prediction: The contour plots, which were carefully established, serve as a valuable tool for delving into the relationship in between both the variables that are dependent and independent illustrated in figures 15 and 16. Specifically, the contour plot relating to particle size highlights that achieving a lower particle size is feasible by maintaining lipid levels between 450 to 700 mg and lipid quantities between 200 to 300 ml. It is noteworthy that optimal entrapment efficacy can be obtained through the strategic utilization of the central composite design approach. Moreover, the CCD point prediction method was instrumental in crafting the NLC dispersion. The precise composition of the dispersion, comprising Stearic acid (700 mg), Isopropyl myristate (300 mg), and lecithin (200 mg), was meticulously determined to ensure the creation of an ideal formulation that meets the necessary criteria for a successful outcome.

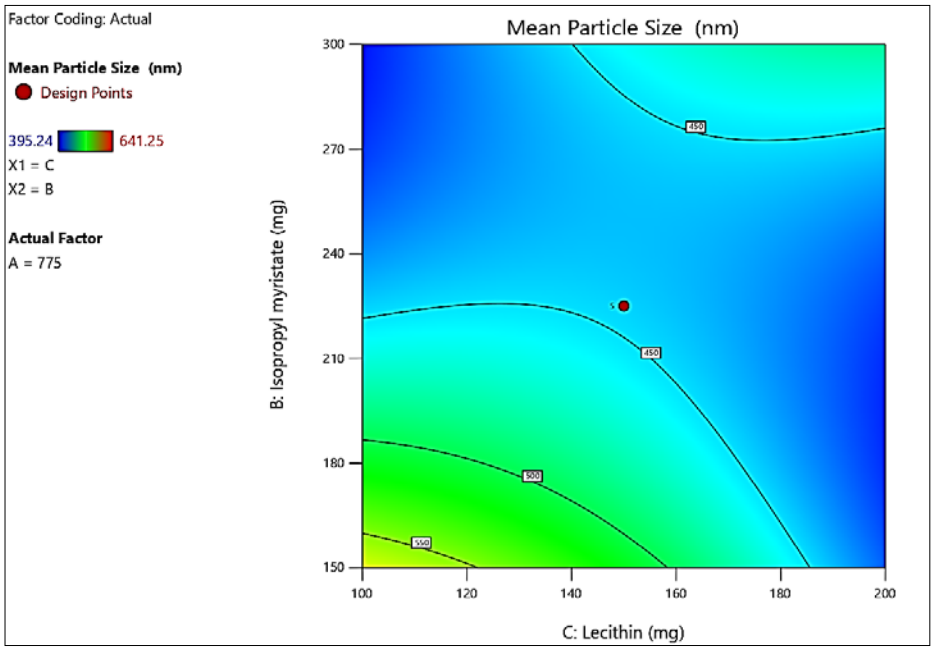

Fig 15: Particle Size of NLC-SN10 Dispersion

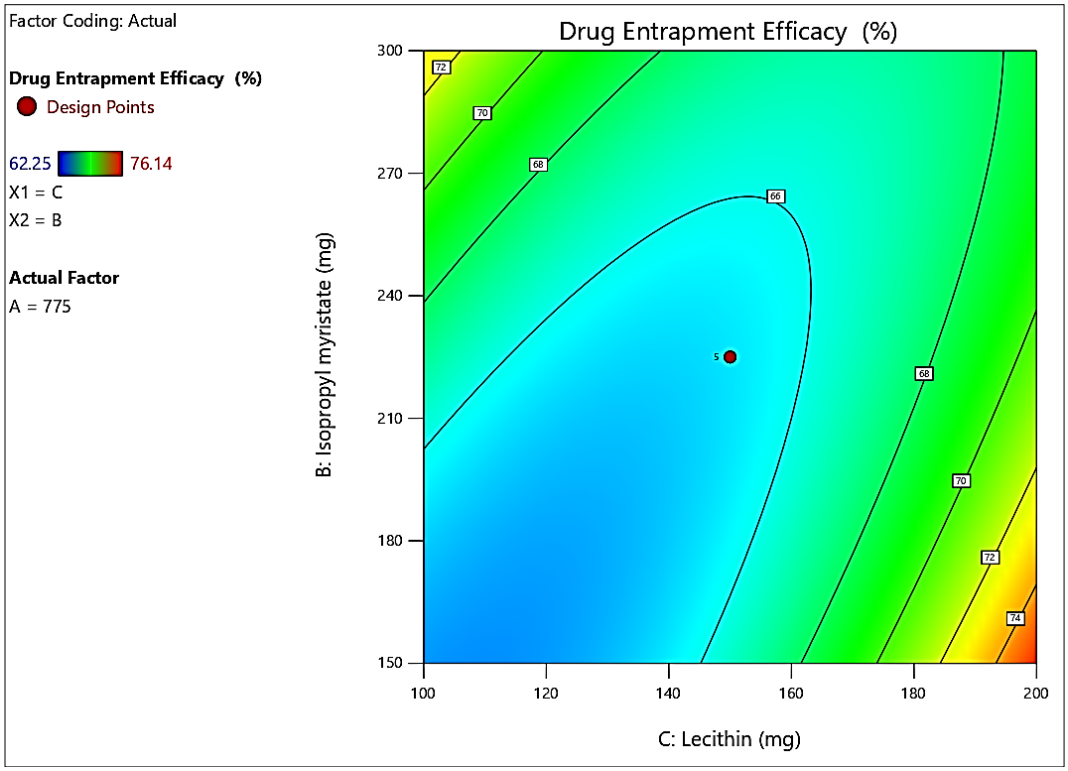

Fig 16: % of EE of NLC-SN10 Dispersion

3.6 SCZ nitrate-NLCs Characterization

3.6.1 Scanning Electron Microscopy

Additional information was gathered through SEM analysis to study the particle size and shape, particularly focusing on spherical and disc-like particles falling within the nanometer range. This data was illustrated in figures 17 and 18, with the size measurements being conducted using Malvern mastersizer. The SEM images revealed clusters of particles, attributable to the carrier's polymorphic nature and the specific sample preparation method used for microscopic assessment. Some particles displayed non-spherical characteristics, possibly linked to the lipid's polymorphic behavior during the heating process as observed in the SEM analysis. This polymorphism effect on particle shape further emphasizes the complexity and variability present in the nano formulation, highlighting the need for detailed analysis and understanding in order to optimize product performance and stability.

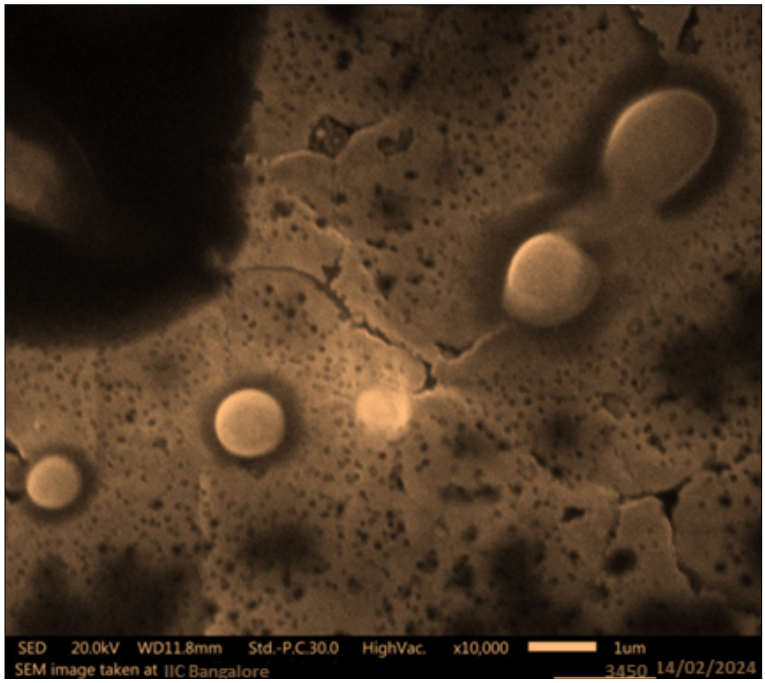

Fig 17: SEM Image of NLC-SN10 Dispersion at 10000x

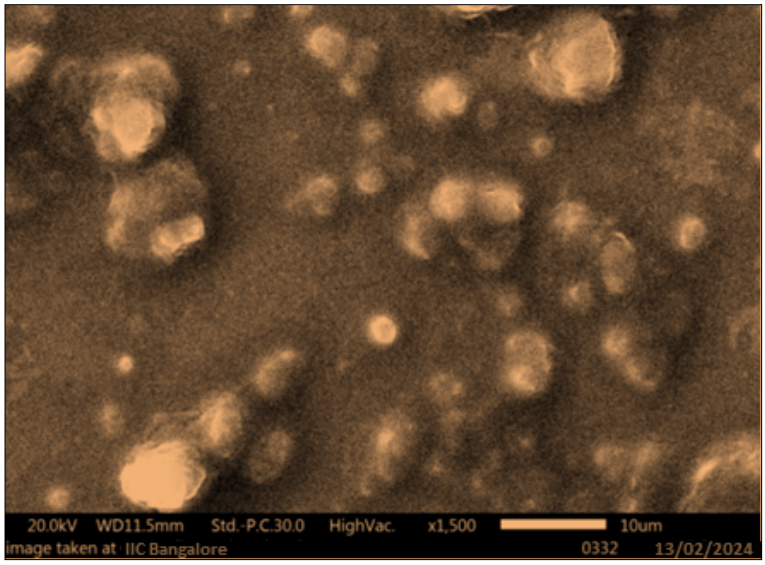

Fig 18: SEM Image of NLC-SN10 Dispersion at 15000x

3.7 Stability Studies of SCZ-NLC

During the conducted stability studies, which followed the guidelines set by the ICH, the data was collected by monitoring the stored formulation over a period of 180 days. The comprehensive analysis revealed that throughout this testing time frame, essential aspects such as the particle size distribution d90%, entrapment efficacy, and zeta potential of the optimized NLC dispersion remained consistent and unchanged. This consistency in the crucial parameters highlights the robust stability of the nano formulation during the duration of the storage period, affirming its reliability and quality under set storage conditions. Table 10 shows the stability studies of SCZ-NLC.

Table 10: Stability Studies of SCZ-NLC

Stability parameters	NLC-SN-9		NLC-SN-10	
	0 Days	180 Days	0 days	180 days
Particle size (d90%)	398±6.251	416±4.270	386±4.551	406±3.982
Zeta potential	-22.1±4.230	-21.0±2.602	-23.4±3.721	-21.8±4.609
% Entrapment	76.15±1.50	72.45±1.10	78.24±1.85	74.35±2.042

4. Conclusion

The current research could show and maximize the NLCs for efficient topical delivery of SCZ, a broad-spectrum activity antifungal drug. Formulation process involved a methodical preformulation screening, lipid screening, and optimization through CCD that resulted in the creation of an optimal NLC-SN10 containing stearic acid, isopropyl myristate, and lecithin. These reagents were chosen due to their high solubilizing activity and SCZ biocompatibility, and their blending was favorable to the creation of stable nano-sized carriers. The best NLC-SN10 formula had desirable physicochemical characteristics, such as particle size of 395.24 ± 2.46 nm, good entrapment efficiency (76.14 ± 1.35%), and a negative zeta potential (−23.85 ± 0.25 mV), all of which are necessary for stability and improved skin permeability. SEM results confirmed spherical, monodisperse particle morphology, which is representative of homogeneity of formulation characteristics. Drug lipid compatibility was confirmed by FT-IR spectral scan to establish the lack of chemical interaction in between excipients and drug. Furthermore, the 180-day stability study once again reaffirmed the stability of the optimized NLC formulation, with essentially no change in zeta potential, particle size, and entrapment efficiency. This assures the efficacy of the SCZ-loaded NLCs for prolonged storage and application. Better drug entrapment and nanoscale particle size indicate better penetration through the stratum corneum, which is an essential barrier to transdermal drug delivery. This functionality is evidence of the capability of NLCs to surpass the challenges of conventional formulations, such as low skin retention and bioavailability. Finally, this study justifies the application of NLC-based drug delivery systems as a promising platform for enhancing the therapeutic activity of antifungal agents such as Sulconazole nitrate. Development and characterization of effective SCZ-NLC not only boosted drug stability and solubilization but also demonstrated potential towards commercial topical antifungal formulations. Future *in vivo* performance studies and clinical validation are needed to establish the clinical utility and therapeutic value of this new NLC-based topical gel formulation.

Abbreviations

API: Active Pharmaceutical Ingredient; BCS: Biopharmaceutics Classification System; DLS: Dynamic Light Scattering; EE: Entrapment Efficiency; FTIR: Fourier Transform Infrared Spectroscopy; HPLC: High-Performance Liquid Chromatography; ICH: International Council for Harmonisation; NLC: Nanostructured Lipid Carrier; PDI: Polydispersity Index; RES: Resveratrol; SEM: Scanning Electron Microscopy; SLN: Solid Lipid Nanoparticles; TEM: Transmission Electron Microscopy; UV: Ultraviolet; ZP: Zeta Potential.

Author Contribution

It is hereby acknowledged that all authors have accepted responsibility for the manuscript's content and consented to its submission. They have meticulously reviewed all results

and unanimously approved the final version of the manuscript.

Human and Animal Rights
Not applicable.

Study limitations
The study was limited to *in vitro* characterization and dissolution testing. *In vivo* correlation data are lacking, making it difficult to establish the pharmacokinetic superiority of the developed formulations.

Acknowledgements
The authors are thankful to the management and Principal of Shri Baba Mastnath Institute of Pharmaceutical Sciences and Research, Rohtak, for their continuous support and motivation.

Consent for Publication
Not applicable.

Funding
None.

Conflict of Interest
The authors declare no conflict of interest financial or otherwise.

References
1. Warnock DW. Trends in the epidemiology of invasive fungal infections. Nihon Ishinkin Gakkai Zasshi. 2007;48(1):1-12.
2. Ghannoum MA, Rice LB. Antifungal agents: mode of action, mechanisms of resistance, and correlation of these mechanisms with bacterial resistance. Clin Microbiol Rev. 1999;12(4):501-517.
3. Elfawal MA, Savinov SN, Aroian RV. Drug screening for discovery of broad-spectrum agents for soil-transmitted nematodes. Sci Rep. 2019;9(1):12347.
4. Tanitame A, Oyamada Y, Ofuji K, Fujimoto M, Suzuki K, Ueda T, Terauchi H, Kawasaki M, Nagai K, Wachi M, Yamagishi J. Synthesis and antibacterial activity of novel and potent DNA gyrase inhibitors with azole ring. Bioorg Med Chem. 2004;12(21):5515-5524.
5. Lee Y, Puumala E, Robbins N, Cowen LE. Antifungal drug resistance: molecular mechanisms in *Candida albicans* and beyond. Chem Rev. 2021;121(6):3390-3411.
6. Riaz A, Hendricks S, Elbrink K, Guy C, Maes L, Ahmed N, Kiekens F, Khan GM. Preparation and characterization of nanostructured lipid carriers for improved topical drug delivery: evaluation in cutaneous leishmaniasis and vaginal candidiasis animal models. AAPS PharmSciTech. 2020;21(5):185.
7. Souto EB, Baldim I, Oliveira WP, Rao R, Yadav N, Gama FM, Mahant S. SLN and NLC for topical, dermal, and transdermal drug delivery. Expert Opin Drug Deliv. 2020;17(3):357-377.
8. Pardeike J, Hommoss A, Müller RH. Lipid nanoparticles (SLN, NLC) in cosmetic and pharmaceutical dermal products. Int J Pharm. 2009;366(1-2):170-184.
9. Patel D, Dasgupta S, Dey S, Ramani YR, Ray S, Mazumder B. Nanostructured lipid carriers-based gel for the topical delivery of aceclofenac: preparation, characterization, and in vivo evaluation. Sci Pharm. 2012;80(3):749-764.
10. Madan JR, Khobaragade S, Dua K, Awasthi R. Formulation, optimization, and in vitro evaluation of nanostructured lipid carriers for topical delivery of apremilast. Dermatol Ther. 2020;33(3):e13370.
11. Singh G, Kumar N, Narwal S, Dhingra AK. Oxidative stress in cardiovascular diseases: mechanisms and exploring advanced therapies. Cardiovasc Hematol Agents Med Chem. 2025.
12. Dushyant, Narwal S, Saini V, Dhingra AK, Singh J, Jasmeen, Devi R, Shabnam. Artificial intelligence in pharmaceutical drug development: transforming formulation and innovation. Curr Drug Discov Technol. 2025.
13. Kasztelanic R, Michalik D, Anuszkiewicz A, Buczynski R. Optimization of the nanostructured weakly coupled few-mode fiber for mode-division-multiplexed systems. Opt Express. 2022;30(23):41832-41846.
14. Fahmy UA, Alaofi LA, Awan ZA, Alqarni HM, Alhakamy NA. Optimization of thymoquinone-loaded coconut oil nanostructured lipid carriers for the management of ethanol-induced ulcer. AAPS PharmSciTech. 2020;21(5):137.
15. Ye Q, Li J, Li T, Ruan J, Wang H, Wang F, Zhang X. Development and evaluation of puerarin-loaded controlled-release nanostructured lipid carriers by central composite design. Drug Dev Ind Pharm. 2021;47(1):113-125.
16. Kanwar R, Gradzielski M, Prevost S, Appavou MS, Mehta SK. Experimental validation of biocompatible nanostructured lipid carriers of sophorolipid: optimization, characterization and in vitro evaluation. Colloids Surf B Biointerfaces. 2019;181:845-855.
17. Müller RH, Mäder K, Gohla S. Solid lipid nanoparticles (SLN) for controlled drug delivery: a review of the state of the art. Eur J Pharm Biopharm. 2000;50(1):161-177.
18. Badalkhani O, Pires PC, Mohammadi M, Babaie S, Paiva-Santos AC, Hamishehkar H. Nanogel containing gamma-oryzanol-loaded nanostructured lipid carriers and TiO_2/MBBT: a synergistic nanotechnological approach for skin protection. Pharmaceuticals (Basel). 2023;16(5):670.
19. Nnamani PO, Ugwu AA, Nnadi OH, Kenechukwu FC, Ofokansi KC, Attama AA, Lehr CM. Formulation and evaluation of transdermal nanogel for delivery of artemether. Drug Deliv Transl Res. 2021;11(4):1655-1674.
20. Jitta SR, Bhaskaran NA, Salwa, Kumar L. Antioxidant-containing nanostructured lipid carriers of ritonavir: development, optimization, and in vitro and in vivo evaluations. AAPS PharmSciTech. 2022;23(4):88.
21. Kakade P, Patravale V, Patil A, Disouza J. Formulation development of nanostructured lipid carrier-based nanogels encapsulating tacrolimus for sustained therapy of psoriasis. Int J Pharm. 2024;660:124172.
22. Han DE, Xin YF, Wei HC, Zhu XL, Liu YM, Tian P. Formulation optimization of emodin nanostructured lipid carriers by Box-Behnken response surface method and in vitro quality evaluation. Zhongguo Zhong Yao Za Zhi. 2022;47(4):913-921.
23. Ho HMK, Craig DQM, Day RM. Design of experiment approach to modeling the effects of formulation and

drug loading on the structure and properties of therapeutic nanogels. Mol Pharm. 2022;19(2):602-615.
24. Ali A, Ali A, Rahman MA, Warsi MH, Yusuf M, Alam P. Development of nanogel loaded with lidocaine for wound healing: illustration of improved drug deposition and skin safety analysis. Gels. 2022;8(8):466.
25. Ramireddy AR, Behara DK. Development and optimization of eberconazole nanostructured lipid carrier topical formulations based on the QbD approach. AAPS PharmSciTech. 2025;26(4):87.
26. Voltan AR, Alarcon KM, Fusco-Almeida AM, Soares CP, Mendes-Giannini MJS, Chorilli M. Highlights in endocytosis of nanostructured systems. Curr Med Chem. 2017;24(18):1909-1929.
27. Gadhave D, Rasal N, Sonawane R, Sekar M, Kokare C. Nose-to-brain delivery of teriflunomide-loaded lipid-based carbopol-gellan gum nanogel for glioma: pharmacological and in vitro cytotoxicity studies. Int J Biol Macromol. 2021;167:906-920.
28. Kesharwani D, Das Paul S, Paliwal R, Satapathy T. Exploring potential of diacerin nanogel for topical application in arthritis: formulation development, QbD-based optimization and pre-clinical evaluation. Colloids Surf B Biointerfaces. 2023;223:113160.